

The main sequence from F to K stars of the solar neighbourhood in SDSS colours

Andreas Just* and Hartmut Jahreiß

Astronomisches Rechen-Institut at ZAH, University of Heidelberg, Mönchhofstraße 12-14, 69120 Heidelberg, Germany

Received XXXX, accepted XXXX

Published online XXXX

Key words (Galaxy:) solar neighborhood, Galaxy: stellar content, stars: fundamental parameters, catalogs

For an understanding of Galactic stellar populations in the SDSS filter system well defined stellar samples are needed. The nearby stars provide a complete stellar sample representative for the thin disc population. We compare the filter transformations of different authors applied to the main sequence stars from F to K dwarfs to SDSS filter system and discuss the properties of the main sequence. The location of the mean main sequence in colour-magnitude diagrams is very sensitive to systematic differences in the filter transformation. A comparison with fiducial sequences of star clusters observed in g', r', i' show good agreement. Theoretical isochrones from Padua and from Dartmouth have still some problems especially in (r-i)-colour.

© 0000 WILEY-VCH Verlag GmbH & Co. KGaA, Weinheim

1 Introduction

The Sloan Digital Sky Survey (SDSS) with sky coverage of almost 10,000 deg² has collected at present the largest and most homogeneous database comprising about 10⁸ stellar objects in the Milky Way. The SDSS photometric system was specifically designed for the survey to provide continuous coverage over the entire optical wavelength range in the five filters $u g r i z$. In the most recent sixth data release (Adelman-McCarthy et al. 2008) the new 'ubercalibration' of the photometry was applied to provide an improved homogeneous relative calibration over the whole survey to 1% in $g r i z$ and 2% in u (Padmanabhan et al. 2008). The zero-points are not exactly in the AB system, but for the $g r i$ filters, the corrections are below 1% and can be neglected. For the zero-points of stars brighter than 14.5 mag see also Chonis & Gascell (2008).

Since most standard stars are too bright to be directly observed with the 2.5 m SDSS telescope, it is a complicated matter to establish standards. One way is to measure the standard stars with a smaller telescope. The SDSS photometric system was originally defined at the 0.5 m photometric telescope (PT) with $u' g' r' i' z'$ (Fukugita et al. 1996). A similar filter set is used in the USNO 1 m telescope for these calibration issues. Since these filters are slightly different from $u g r i z$ at the main 2.5 m telescope (Abazajian et al. 2003), transformation formulas from $u' g' r' i' z'$ to $u g r i z$ must be established (Tucker et al. 2006).

Despite the enormous wealth of information that the SDSS database provides the majority of current observational and theoretical knowledge of resolved stellar populations is based largely on the Johnson-Kron-Cousins $U B V R_C I_C$ photo-

metric system and some other systems such as the Strömgren, DDO, Vilnius, and Geneva systems.

The best way of calibrating the theoretical isochrones is the observation of fiducial isochrones of simple stellar populations (SSP) with known age and metallicity in SDSS filters. Clem, VandenBerg, & Stetson (2008) obtained fiducial stellar population sequences for the $u' g' r' i' z'$ photometric system from a number of different Galactic star clusters, spanning a wide range in metallicity and magnitude. In order to achieve the required accuracy they have first established a new set of secondary standard stars in selected open and globular star clusters for this photometric system (Clem, VandenBerg, & Stetson 2007).

For a physical understanding of observed stellar populations is essential to interpret the data via stellar evolution tracks or isochrones. Girardi et al. (2004) were the first, who provided tables of theoretical isochrones in $u g r i z$ derived from stellar spectra. These have however turned out to lack the necessary precision to correctly interpret different stellar populations from the SDSS database. Recently in the Dartmouth Stellar Evolution Program (Dotter et al. 2007, 2008) isochrones in $u g r i z$ are presented based on VandenBerg & Clem (2003) and Ivezić et al. (2007).

The solar neighbourhood provides a complete stellar sample of the Milky Way disc with measured absolute magnitudes from Hipparcos data and the Catalogue of Nearby Stars (CNS4, Jahreiß & Wielen 1997). Therefore it is a unique place for investigating the properties of the stellar disc population testing the transformations to the SDSS filters. The purpose of this paper is to transform the CNS4 absolute luminosities in ($M_B M_V M_{R_C} M_{I_C}$) of main sequence (MS) stars to the SDSS luminosities ($M_g M_r M_i$), and to derive the corresponding colour-magnitude relations.

* Corresponding author: e-mail: just@ari.uni-heidelberg.de

In the next section we present the filter transformations of different authors. In Sect. 3 the selection of the stellar sample and the available colours are presented. In Sect. 4 we discuss the differences of the various transformation formulas. In Sect. 5 we derive the MS properties for F-K stars and discuss the uncertainties due to different transformations. A comparison with observed fiducial isochrones is also presented and the local stellar number density in $g-r$ space is derived. In Sect. 6 a comparison with theoretical isochrones in the colour magnitude diagrams (CMD) is given. The results are summarized in Sect. 7.

2 Filter transformations

Several groups have derived photometric transformations of the SDSS photometric system to the $UBVR_C I_C$ system or vice versa. Smith et al. (2002) defined the $u'g'r'i'z'$ photometric system on 158 standard stars, a subset of $UBVR_C I_C$ standard stars from Landolt (1992), using the USNO-1.0m telescope. They derived transformation formulas from $UBVR_C I_C$ to $u'g'r'i'z'$. Rodgers et al. (2006) refined this work by including only MS stars into the transformation calculation and using a second-order polynomial in $(B-V)$ for g' as well as bilinear equations including two colours, where the corresponding filters overlap, i.e. $B-V$ and $V-R_C$ for calculating $g'-r'$. Bilir, Karaali, & Tunçel (2005) also improved the transformations of Smith et al. (2002) by restricting the stellar sample to population I stars and checking the stellar locus in the 2-colour diagram ($g-r, r-i$) by comparing with a sample of nearby Hipparcos stars.

Jordi, Grebel, & Ammon (2006) have derived the colour transformation for main sequence stars directly for the 2.5m SDSS telescope $ugriz$ photometric system by including the faint extension of standard stars from Stetson (2000). Separate transformation formulas were derived for population I and II stars. Chonis & Gaskell (2008) derived linear transformations from $griz$ to $BVR_C I_C$ using the Landolt and Stetson standard stars, which are inverted for our purposes. They also showed the consistency with the transformations of Jordi et al. (2006).

Ivezić et al. (2007) derived nonlinear functions for the transformations from $griz$ to $BVR_C I_C$. Recently Bilir et al. (2008) have calculated transformations between the SDSS photometry and the 2MASS photometry as well as between the $UBVR_C I_C$ photometry and the 2MASS photometry for different metallicity ranges.

We compare the results of four different transformations, namely of Bilir et al. (2005) labeled by B05, of Jordi et al. (2006) J06, of Rodgers et al. (2006) R06, and of Chonis & Gaskell (2008) C08. Since B05 and R06 are both improvements of the transformations of Smith et al. (2002) labeled by S02, we do not include S02 in the investigation. The transformations of Ivezić et al. (2007) are not included, because they cannot easily be inverted due to the higher-order terms. Applying the transformations of Bilir et al. (2008)

via the 2MASS photometry without taking 2MASS data of the stellar sample into account seems also not reasonable.

We cannot claim at the present status of our investigations, which of the transformations should be preferred. The transformation formulas for M_g and $g-r$ of B05 and C08 can be applied without further approximations to the complete stellar sample, because only M_V and $B-V$ are required. For convenience and clarity in the comparisons of the different transformations we select the C08 transformation as fiducial.

In J06 we use the transformations for population I stars, where we combined the transformations for $g-V$ and $r-R$ to derive an equation for $g-r$ as a function of $B-V$ and $V-R_C$ instead of using the simple equation for $g-r$ given in their table. The stellar locus in the 2-colour diagram ($B-V, V-R_C$), where these equations are consistent to each other, is shown in Fig. 12.

The transformations R06 are originally to the primed system and must be converted to the unprimed system.

Throughout the paper we convert all colours from the $u'g'r'i'z'$ to the $ugriz$ system, if necessary, by applying

$$\begin{aligned} g &= g' + 0.060[(g' - r') - 0.53] \\ r &= r' + 0.035[(r' - i') - 0.21] \\ i &= i' + 0.041[(r' - i') - 0.21] \end{aligned} \quad (1)$$

from Tucker et al. (2006) leading to

$$\begin{aligned} g-r &= 1.060(g'-r') - 0.035(r'-i') - 0.024 \\ r-i &= 0.994(r'-i') + 0.001 \end{aligned} \quad (2)$$

Note, that transformations via the primed system lead to additional colour terms in the unprimed system, i.e. $(V-R_C)$ -terms for g and $g-r$ and also a $(R_C - I_C)$ -term in the formula for $g-r$.

All transformations can be written in the general form

$$\begin{aligned} g-V &= a_1(B-V)^2 + b_1(B-V) + c_1(V-R_C) + d_1 \\ g-r &= a_2(B-V) + b_2(V-R_C) + c_2(R_C - I_C) + d_2 \\ r-i &= a_3(R_C - I_C) + b_3 \end{aligned} \quad (3)$$

The coefficients of B05, J06, R06, and C08 are listed in Table 1 with the coefficients of S02 (Smith et al. 2002) added for comparison.

3 Nearby stars

We start with a volume complete sample of nearby stars selected from Hipparcos stars and the CNS4 to the completeness limit in magnitude bins of M_V . Due to the Hipparcos survey the limiting distances are 200, 100, 75, 50, 30, 25 pc in the magnitude ranges < 0.5 , 1 ± 0.5 , 2 ± 0.5 , 3 ± 0.5 , 4 ± 0.5 , and 7 ± 2.5 mag, respectively. The CMDs in Hipparcos colours ($B-V, M_V$) and in ($g-r, M_g$) using C08 are shown in Fig. 1. Here fainter stars are included in order to show the turnover of the MS to the M dwarfs. The transformations C08 are valid only for $0.4 < B-V < 1.5$. The

Table 1 Coefficients of the transformation formulas given in Eqs. 3 of the different authors. The first 3 rows refer to the calculated quantity, the contributing terms and the coefficients, respectively. Column 1 gives the source, and the other columns the coefficient, if the terms appear in the corresponding equation. In the notes the validity ranges are also given.

formula term coeff.	$M_g - M_V$				$g-r$				$r-i$	
	$(B-V)^2$	$(B-V)$	$(V-R_C)$	cnst.	$(B-V)$	$(V-R_C)$	(R_C-I_C)	cnst.	(R_C-I_C)	cnst.
	a_1	b_1	c_1	d_1	a_2	b_2	c_2	d_2	a_3	b_3
C08	–	0.642	–	–0.135	1.094	–	–	–0.248	0.939	–0.198
R06	–0.042	0.619	0.079	–0.133	0.295	1.365	–0.035	–0.249	0.994	–0.210
J06	–	0.643	–	–0.127	0.643	0.725	–	–0.213	0.988	–0.221
B05	–	0.634	–	–0.108	1.124	–	–	–0.252	1.04	–0.224
S02	–	0.60	–	–0.11	1.039	–	–0.035	–0.218	0.994	–0.21

C08: Chonis & Gascall (2008): $0.08 < r-i < 0.5$ and $0.2 < g-r < 1.4$

R06: Rodgers et al. (2006): $-0.2 < B-V < 1.6$

J06: Jordi et al. (2006): $g-r$ for $(V-R_C) \leq 0.93$

B05: Bilir et al. (2005): $0 < B-V < 1.4$

S02: Smith et al. (2002): $-0.3 < B-V < 1.9$ (and $R_C-I_C \leq 1.15$ for $r'-i'$)

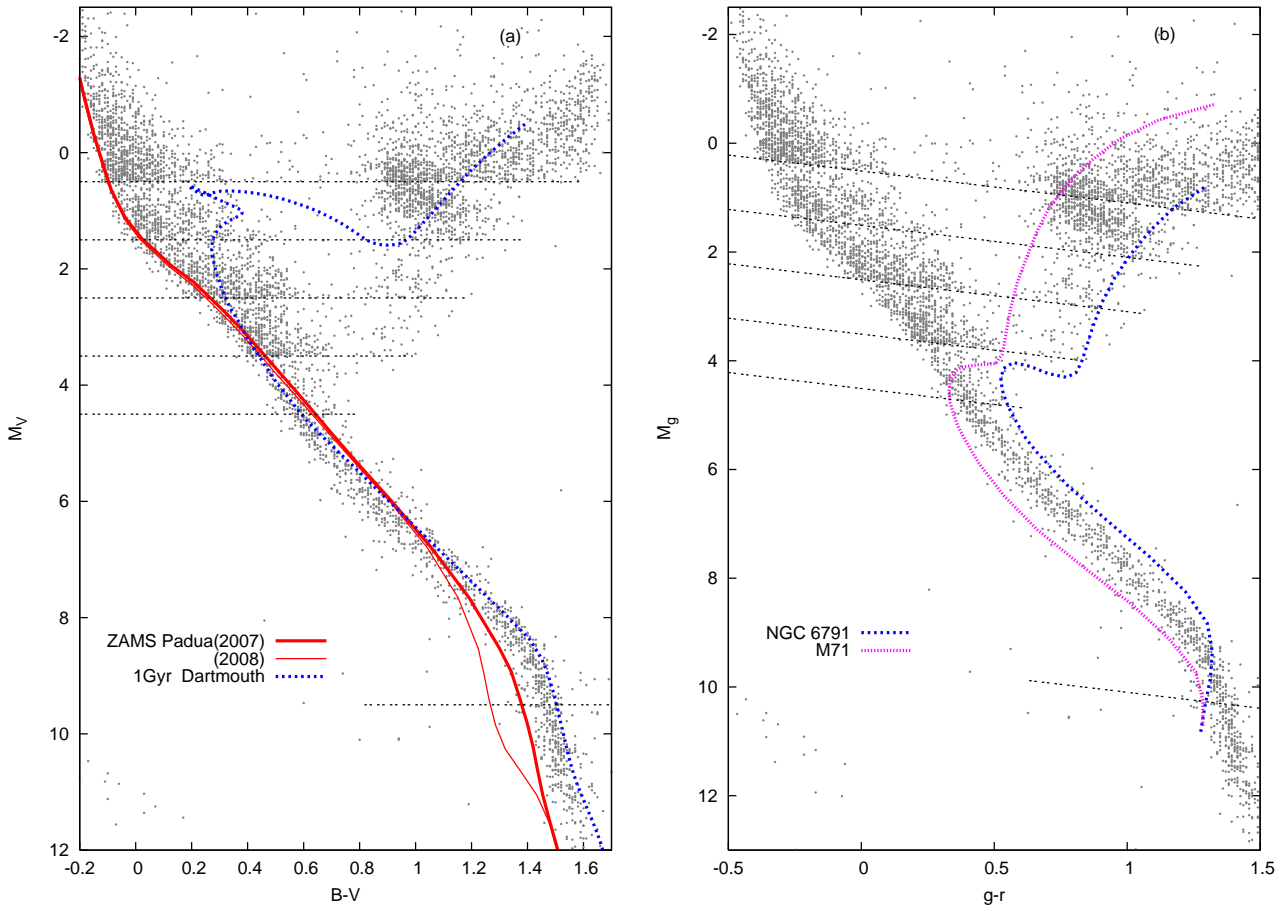


Fig. 1 CMDs in $(B-V, M_V)$ and $(g-r, M_g)$, where the transformation C08 was used (Chonis & Gascall 2008), for volume-selected Hipparcos stars (grey dots; see Sect. 3). The completeness distances are 200, 100, 75, 50, 30, 25 pc in the magnitude ranges $< 0.5, 1 \pm 0.5, 2 \pm 0.5, 3 \pm 0.5, 4 \pm 0.5,$ and 7 ± 0.5 mag, respectively. In (a) the ZAMS from Padua (old: thick line, new: thin line) and the 1 Gyr isochrone from Dartmouth with metallicity $[\text{Fe}/\text{H}] = +0.13$ (see Sect. 6) are overplotted. In (b) the ridge lines of the star clusters NGC 6791 and M71 are shown.

extrapolation to the blue and red part as well as to the giants must be used with caution.

For the detailed investigation of the local MS from F to K dwarfs we use the data from the Catalogue of Nearby Stars (CNS4). All stars are also in the Hipparcos catalogue, but the luminosities and colours given in the CNS4 rely on more thoroughly collected photometric data than from the Hipparcos data alone.

F to K stars were selected from the CNS4 according to $0.30 \leq B - V \leq 1.35$ with parallaxes larger than 40 mas. We removed stars more than 0.8 mag above and below the estimate mean MS in order to avoid contamination by turnoff stars, giants and white dwarfs. After removing additionally a few stars with poor photometry there remained 786 dwarf stars. We use this stellar sample as a complete sample of MS stars from F to K type inside a sphere with 25 pc radius. M_V , $B - V$, $V - R$, $R - I$ from the CNS4 catalogue and $g - r$, $r - i$, M_g from the C08 transformation is given as online material for these stars. The first few lines are shown in Table 2.

From these 786 stars 561 stars have not only a $B - V$ colour but also $V - R_C$ and $R_C - I_C$ colours. We use this subsample as representative for the locus of the MS in the solar neighbourhood. For 119 stars $R_C - I_C$ is missing, for 6 stars $V - R_C$ is missing, and 100 stars both colours are missing.

4 Transformation differences

We use the subsample of 561 stars with M_V , $B - V$, $V - R_C$, $R_C - I_C$ as representative for the properties of the MS in the solar neighbourhood. In order to measure the sensitivity of the CMDs on the transformation formulas we apply all transformations C08, R06, J06, and B05 (Chonis & Gascall 2008, Rodgers et al. 2006, Jordi et al. 2006, Bilir et al. 2005) collected in Table 1 to the same stellar sample and compare the results.

We use the transformations C08 as reference. In Figs. 2 - 5 the differences of the transformations are plotted. The differences between the other pairs of transformations can be deduced from the differences of the values in the two corresponding plots with respect to C08.

In M_g (Fig. 2) the systematic differences along the MS are below 0.06 mag. The scatter in the plot for R06-C08 is exclusively due to the transformation from the primed to the unprimed filter system. The differences in the colour index $g - r$ (Fig. 3) show a systematic variation of the same order as for Δg , but with a different $B - V$ dependence. For the R06 and J06 transformations the scatter arises from the $V - R_C$ dependence of $g - r$ and is much larger (up to 0.3 mag). In M_r (Fig. 4) the variation and scatter is comparable to that in $g - r$. In $r - i$ (Fig. 5) there is only a linear trend up to 0.08 mag due to the simple transformation equations in all cases.

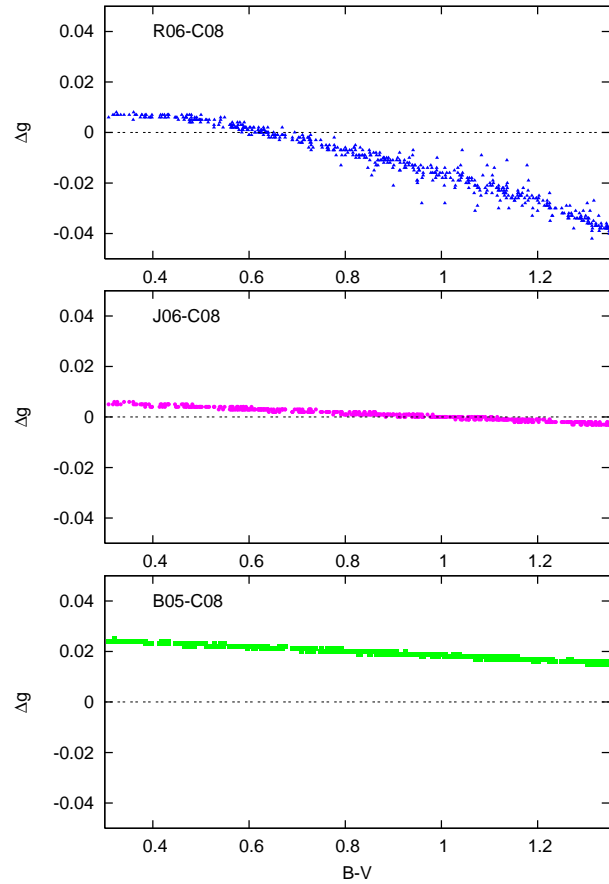


Fig. 2 Comparison of the different transformations relative to C08. The difference in M_g magnitude for the 561 F- to K-dwarfs with all colours in B,V,R,I of the initially selected 786 stars is plotted as a function of $B - V$.

In total the variations in colour by the different transformations will have a much stronger influence on the location of the MS than the variations in the luminosities.

5 The main sequence for F to K dwarfs

The position of the MS in the CMDs and in the 2-colour diagrams are important for estimating the distance of a stellar population and their properties like age and metallicity. The MS in the solar neighbourhood shows a considerable width due to the spread in age and metallicity and the contamination by binary stars. No clear maximum in the magnitude bins exists (ridge line). Therefore we determine a mean MS and measure the width in the CMDs and in the 2-colour diagrams.

The comparison with independent determinations of the MS are necessary for judging the quality of the different transformations. We use the fiducial stellar sequences in $g' r' i'$ of two star clusters from Clem et al. (2007, 2008) transformed to $g r i$. The old open star cluster NGC 6791 has a metallicity of $[\text{Fe}/\text{H}] = +0.40$ and the reddening is $E(B -$

Table 2 First lines of the table with luminosities and colours of the complete sample of 786 stars in the 25 pc sphere. Column 1 is the Hipparcos number, column 2–4 are $g - r$, $r - i$, M_g from the C08 transformation, column 5–8 are M_V , $B - V$, $V - R$, $R - I$ from the CNS4 catalogue, and column 9 is the CNS identifier; suffix A and B denotes components of binaries. The full table is available as online material with ‘—’ as separators.

Hip	$g - r$	$r - i$	M_g	M_V	$B - V$	$V - R$	$R - I$	CNS
sun	0.459	0.114	5.110	4.83	+0.646	0.354	0.332	1
171	0.484	0.186	5.684	5.39	+0.669	0.409	0.409	19140A
436	0.915	0.320	8.017	7.47	+1.063	0.636	0.552	1 30
518	0.501		5.135	4.83	+0.685	0.380		1 41A
544	0.575		5.788	5.44	+0.752	0.410		1 50
910	0.267	0.074	3.637	3.47	+0.471	0.305	0.290	1 100
950	0.238		3.710	3.56	+0.444			4 15
1031	0.600		6.043	5.68	+0.775			22001
...								

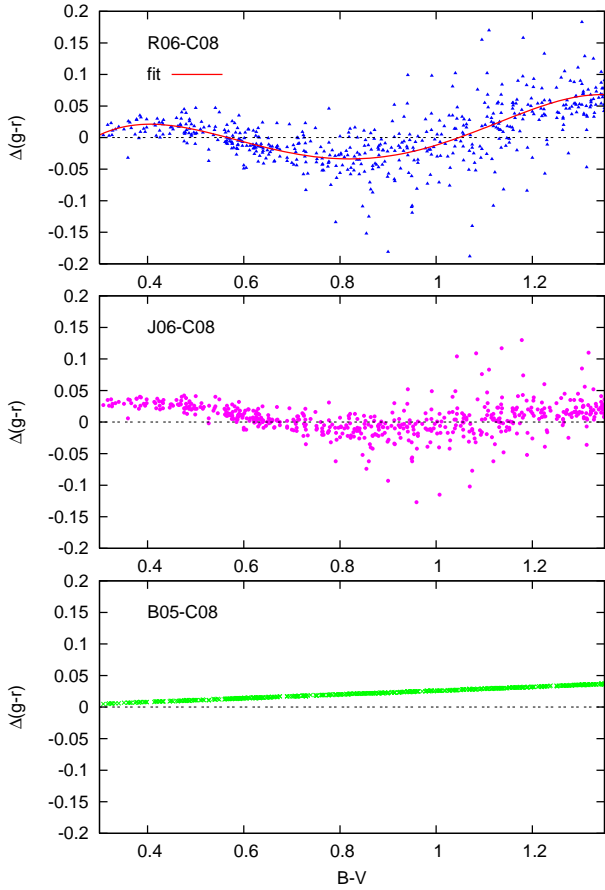


Fig. 3 Same as in Fig. 2 but for $g - r$. The full line in the upper plot is the best fit used for deriving the local number density as a function of $g - r$.

V)=0.155 (Clem et al. 2007). The age of 8 Gyr and distance modulus of $m - M = 13.17$ are taken from Carraro et al. (2006). For the globular cluster M 71 with metallicity $[\text{Fe}/\text{H}]=-0.58$ reddening and distance modulus are still under debate. We use $m - M = 12.89$ and $E(B - V) = 0.25$ derived from $E(J - K) = 0.13$ of Kyeong, Byun, & Chun

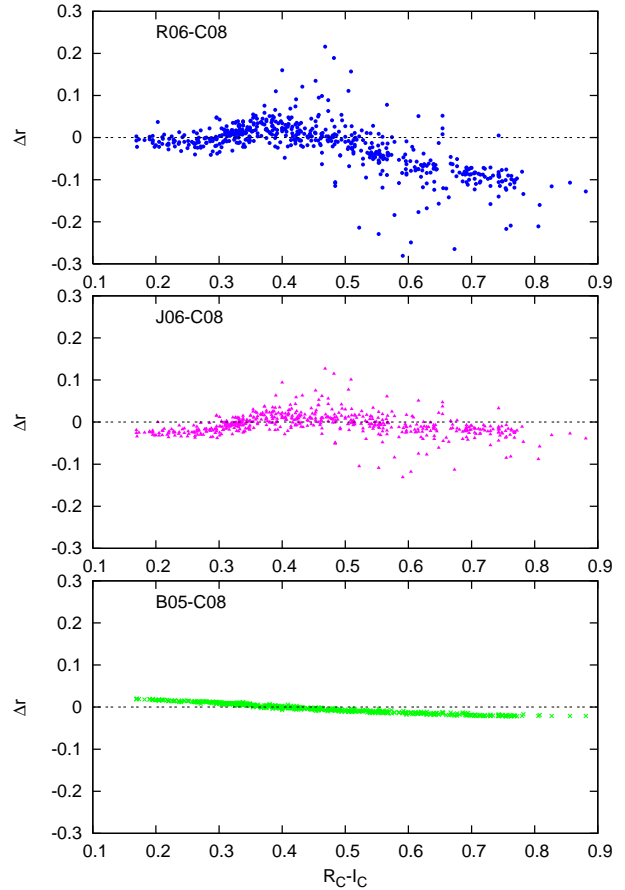


Fig. 4 Same as in Fig. 2, but for M_r .

(1997) using NIR photometry. These star clusters bracket the metallicity range of disc stars in the solar neighbourhood. Therefore the ridge lines of these simple stellar populations (SSP) should be comparable to the boundaries of the local MS.

Fig. 1 shows a general consistency of the C08 transformation with the ridge lines of NGC 6791 and M 71 for F to K stars. In the regime of M dwarfs there appears a dis-

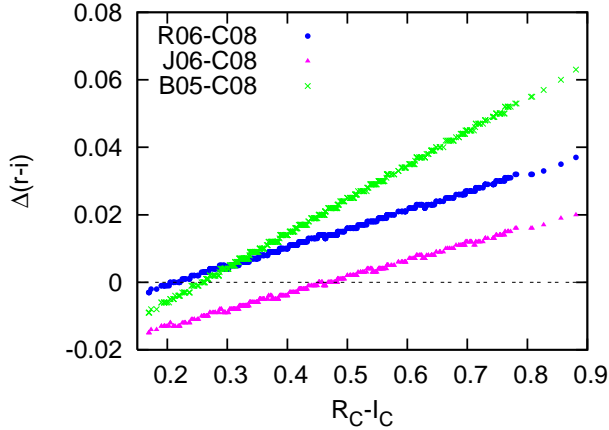


Fig. 5 Same as in Fig. 3 but for $r - i$.

Table 3 Mean MS $M_g(g - r)$ in 0.05 mag bins with the C08 transformation for the complete sample of 786 stars in the 25 pc sphere. First column is $g - r$, second column mean M_g , third column the standard deviation in M_g and column four the number of stars in the 0.05 mag bins.

$g - r$	M_g	σ_g	N	$g - r$	M_g	σ_g	N
0.10	2.72	0.23	11	0.70	6.49	0.32	45
0.15	3.05	0.30	14	0.75	6.72	0.29	41
0.20	3.39	0.26	17	0.80	6.93	0.24	40
0.25	3.73	0.30	25	0.85	7.16	0.25	32
0.30	4.12	0.39	33	0.90	7.39	0.29	35
0.35	4.49	0.39	31	0.95	7.62	0.27	29
0.40	4.82	0.30	53	1.00	7.85	0.29	41
0.45	5.09	0.30	58	1.05	8.08	0.20	30
0.50	5.38	0.30	32	1.10	8.32	0.22	21
0.55	5.69	0.36	39	1.15	8.55	0.23	28
0.60	5.97	0.26	36	1.20	8.80	0.27	38
0.65	6.24	0.34	41				

crepancy. But here we are outside the valid colour regime of C08 and the star cluster fiducial end.

5.1 Colour-magnitude diagrams

The mean absolute magnitudes M_g as a function of $g - r$ is determined by LOWESS (Cleveland 1981) carrying out a robust locally weighted regression, where the amount of smoothing is determined by a parameter f (in our case $f = 0.2$), which describes the fraction of points used to compute each fitted value. The result of C08 is presented in Table 3.

The results for all transformations are shown in Fig. 6 for $(g - r, M_g)$ and in Fig. 7 for $(r - i, M_r)$. Dots are the 561 stars and the full line is the mean MS. Overplotted are the fiducial colour magnitude sequences for the star clusters M71 and NGC 6791 from Clem & Vandenberg (2008) with metallicities $[\text{Fe}/\text{H}] = -0.58$ and $+0.40$, respectively.

The upper left panel of Fig. 6 shows the C08 transformation. In $(g - r, M_g)$ the ridge lines of M71 and NGC 6791 bound nicely the local MS stars. The other three panels

show the same using the transformations R06, J06, and B05, respectively. There is also a general agreement with the star cluster fiducial. Only for R06 there are some outliers at the red and metal rich end.

In the lower panel the mean main sequences from the different transformations are compared. The difference of the C08 transformation using the complete sample of 786 stars to that with 561 stars show the uncertainty due to incompleteness. The differences are below 0.05 mag. The deviations from different transformations are up to 0.5 mag. This corresponds to systematic distance errors of 25%, when applying the distance modulus to observed apparent magnitudes.

In $(r - i, M_r)$ (Fig. 7) there is a clear disagreement above the MS for all transformations. The trends of the mean main sequences are smaller than in $(g - r, M_g)$.

The dashed lines in the upper left panels of Figs. 6 and 7 show the MS with the bright normalization used in Jurić et al. (2008, JIB08) for comparison. In $(r - i, M_r)$, where the MS is originally defined, it fits the data better than in $(g - r, M_g)$. The locus confirms that the 'bright' MS represents the local stellar population with mean metallicity $[\text{Fe}/\text{H}] \approx -0.2$. The offset to the metal poor regime for F stars is expected, because metal poor F stars have a lifetime considerably shorter than the age of the stellar disc. Therefore these old F stars are already in the turnoff phase.

5.2 2-colour diagrams

Since 2-colour diagrams are independent of distance, they are a valuable tool to investigate the intrinsic properties of the stellar populations. In Fig. 8 we show the $(g - r, r - i)$ diagrams for all four transformations compared to the ridge lines of the star clusters NGC 6791 and M71. The transformations C08 and B05 are well bounded by the star cluster fiducials, whereas the transformations R06 and J06, which use a $(V - R)$ -term in the colour transformation for $g - r$, show some outliers at the lower right. Full lines are the mean MS, which are compared directly in the lower plot. Additionally the stellar locus JIB08 of Jurić et al. (2008) showing a small offset to the lower metallicity regime.

5.3 Local normalization

In order to determine the population at the MS as function of colour $g - r$ a complete stellar sample is needed. With C08 applied to the complete stellar sample of 761 stars in the 25 pc sphere we derive the number of stars per 0.05 mag bin in $g - r$. The histogram in Fig. 9 shows the result for a selected position of the binning. Errorbars are \sqrt{N} noise. The full line gives the running mean, which show the sensitivity with respect to the chosen binning.

In order to investigate the sensitivity of the number density function on the filter transformation, we derived $N(g - r)$ also for R06. Since only 561 stars have all colours, we determine M_g and $g - r$ for the other stars in an approximate way. For the 119 stars with $V - R_C$ we estimate $g - r$

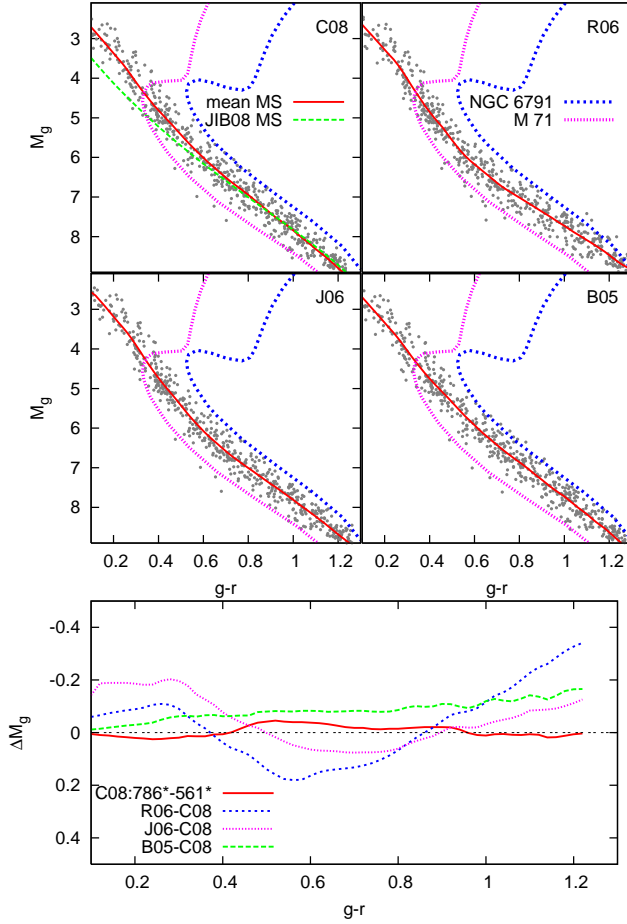


Fig. 6 CMDs for 561 F- to K-dwarfs within 25 pc in $(g-r, M_g)$. Upper panels: CMDs using the different transformations as noted. The fiducial colour magnitude sequences for NGC 6791 and M71 are shown for comparison. The full lines give the mean MS derived with the smoothing algorithm. For comparison the MS with the bright normalization (JIB08) used in Jurić et al. (2008) is plotted in the upper left panel. Lower panel: Differences of the mean MS derived with the different transformation formulas with respect to C08 (561 stars). The difference of the C08 transformation using the complete sample of 786 stars is also shown.

from $g' - r'$ using an approximation from the stellar locus in the 2-colour diagram $(g' - r', r' - i')$ for the 561 stars. The linear best fit of these stars is

$$r' - i' = (0.470 \pm 0.004)(g' - r') - 0.086 \pm 0.0035 \quad (4)$$

for $g' - r' \leq 1.4$

leading to

$$g - r \approx 1.044(g' - r') - 0.021 \quad (5)$$

(6)

instead of Eq. 2. For the remaining 106 stars we use the transformation of C08 and correct M_g and $g - r$. For the correction we determine a fourth order polynomial best fit of $\Delta(g - r)$ (Fig. 3) and add that to the individual values

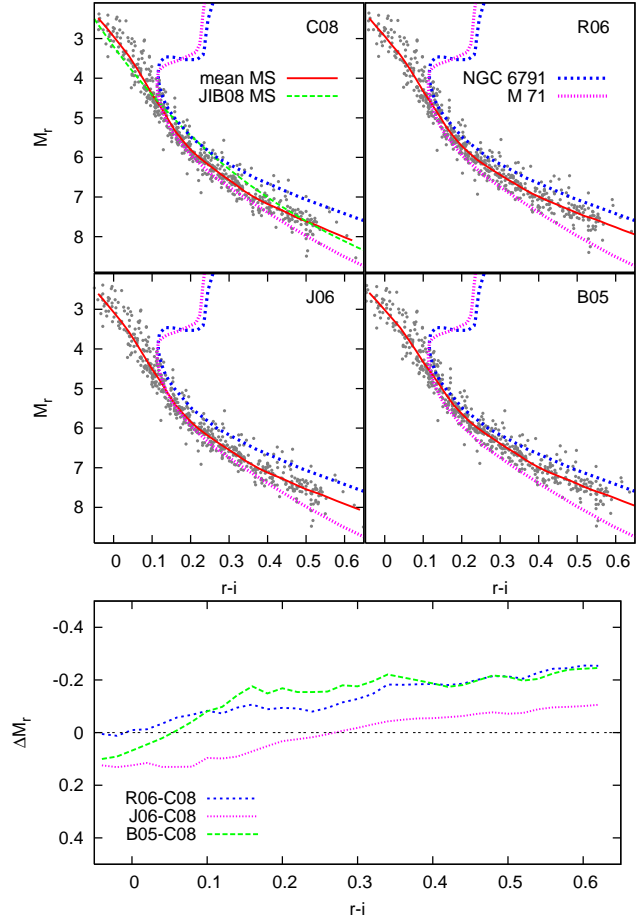


Fig. 7 Similar plots as in Fig. 6 but in $(r-i, M_r)$.

from C08 of the stars. For testing the method, we applied the same method to the subsample of 561 stars with all colours and compared the resulting histograms with these of the R06 transformation. The differences are well below the uncertainty due to noise.

The dashed line shows the car-box average with the R06 transformation. There are systematic differences (higher maximum, lower level at the red end), but they are not significant due to the small number statistics.

The applications of the local number densities are twofold. Firstly they can be used for disc models from star counts as the local normalization. Secondly the local colour distribution can be used to understand the physical properties of the stellar population in the solar neighbourhood. The steep increase at the blue end ($g - r < 0.45$) is due to the increasing lifetime of the stars with decreasing stellar mass until the age of the disc is reached. This effect is reduced by the increasing scale height of the stars with increasing mean age. The shape of the density function in the red part ($g - r > 0.45$) is determined by a combination of the IMF and of the stellar mass-colour relation, which depends on the metallicity.

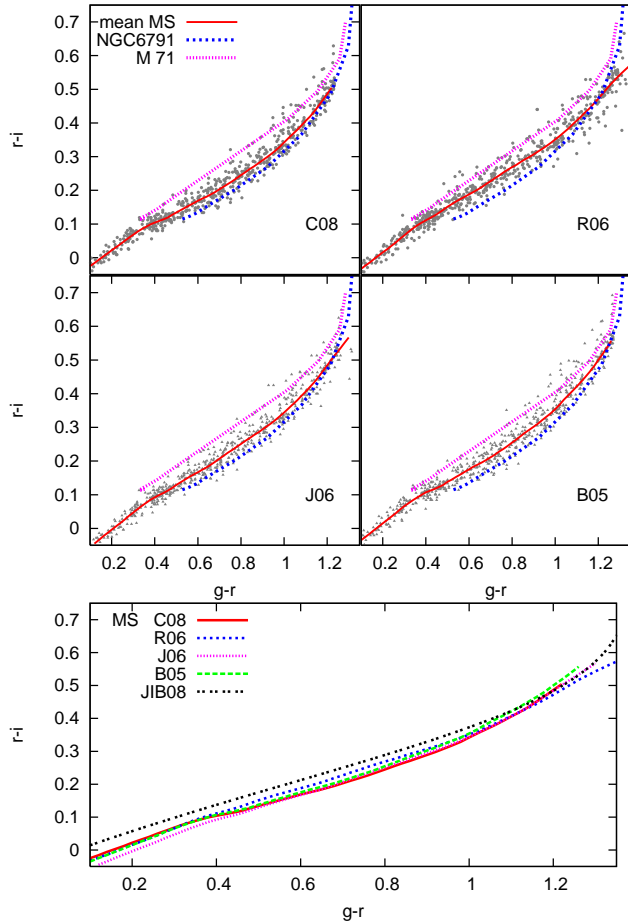


Fig. 8 The upper panels show similar plots as in Fig. 6 but in $(g-r, r-i)$. The lower panel shows a direct comparison of the mean MS of the different transformations. The stellar locus of Jurić et al. (2008 JIB08) is also shown.

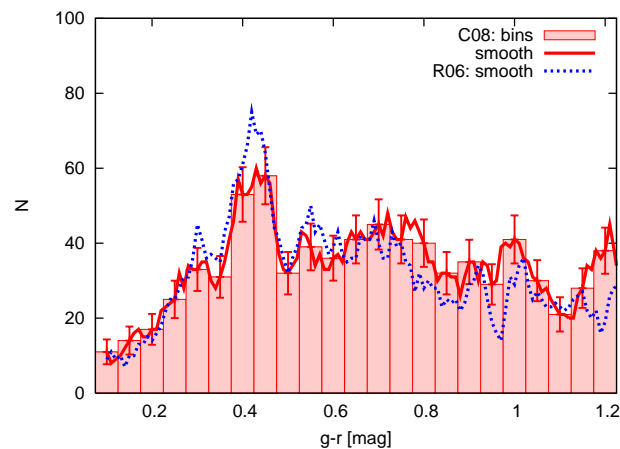


Fig. 9 Local number density in the 25 pc sphere in $g-r$ bins of 0.05 mag. The histogram and full line show the data with the transformation C08 of Chonis & Gascall (2008). The errorbars show the 1σ noise error. The dashed line is the result using the R06 transformation of Rodgers et al. (2006) with the completeness corrections as discussed in the text.

6 Isochrones

For an understanding of the physical properties of stellar populations a comparison with theoretical isochrones is very useful. Here we compare the data with two different sets of isochrones, where SDSS colours are available and which are provided via a web interface. The Padua isochrones¹ were based until recently on the evolutionary tracks of Girardi et al. (2002). For the SDSS colours see Girardi et al. 2004. Since 2008 new isochrones based on Marigo et al. (2008) are provided via the web interface.

The Dartmouth Stellar Evolution Database² provides different sets of isochrones in $B V R_C I_C$. We use the isochrones of Vandenberg & Clem (2003). In $ugriz$ the isochrones are based on the Sixth data release of SDSS (Adelman-McCarthy et al. 2008). The parameter grid in age is in steps of 0.5 Gyr starting at an age of 1 Gyr. We use solar $[\alpha, \text{Fe}]$ ratio and normal Helium abundance in our investigation.

In Fig. 1 we compare the old and new Padua ZAMS (zero age main sequence = 1 Myr isochrone) with metallicity $[\text{Fe}/\text{H}] = +0.13$ in $(B-V, M_V)$ with the CMD of the full Hipparcos sample. There is good agreement in the blue and intermediate colour regime. At the red end the isochrones are too blue/faint. The new isochrones (thin lines, labeled 2008) are inferior to the classical isochrones (2007). The Dartmouth isochrone of 1 Gyr matches the MS very good down to the M dwarfs.

A detailed comparison of the isochrones with the local stellar population transformed with C08 is shown in Figs. 10 - 12. For Padua we show the ZAMS with $[\text{Fe}/\text{H}] = +0.13$ (as in Fig. 1) and the isochrone of age 12 Gyr with $[\text{Fe}/\text{H}] = -0.55$. For Dartmouth we use the isochrones of age 1 Gyr with $[\text{Fe}/\text{H}] = +0.13$ and of age 12 Gyr with $[\text{Fe}/\text{H}] = -0.55$. The upper panels show in $(B-V, M_V)$ (Fig. 10), $(R_C - I_C, M_{R_C})$ (Fig. 11), $(B-V, V - R_C)$ and $(B-V, R_C - I_C)$ (Fig. 12), where discrepancies in the Johnson-Cousins system are still present. In $(B-V, V - R_C)$ a number of stars scatter considerably around the MS, which is not the case in $(B-V, R_C - I_C)$. This may be due to observational errors in $V - R_C$. In $(B-V, R_C - I_C)$ the Dartmouth isochrones are systematically offset to the red in $(R_C - I_C)$. Also the colour width due to the metallicity spread is too small.

The lower panels show similar diagrams in SDSS filters, namely $(g-r, M_g)$ (Fig. 10), $(r-i, M_r)$ (Fig. 11), and $(g-r, r-i)$ (Fig. 12).

In $(g-r, M_g)$ both sets of isochrones match the data with the C08 transformation roughly. For G-K stars the Padua isochrones are better at the metal rich edge (bright/red), whereas the Dartmouth isochrones are slightly better in the transition regime from K to M dwarfs. In $(r-i, M_r)$ the consistency is much worse. There are significant offsets of both sets of isochrones. The Padua isochrones are too faint/blue and the Dartmouth isochrones are too bright/red.

¹ <http://stev.oapd.inaf.it/cmd>

² <http://stellar.dartmouth.edu/models/index.html>

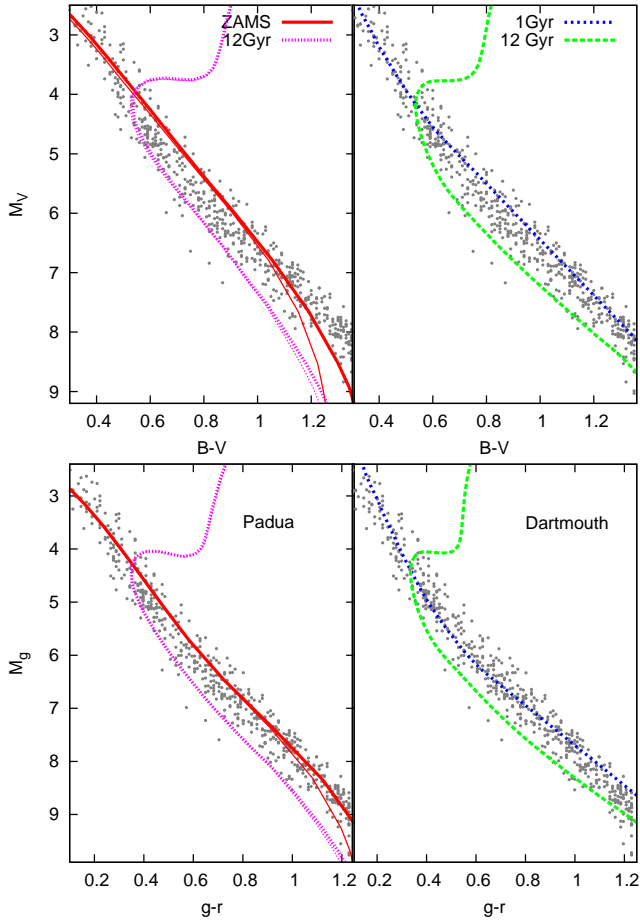


Fig. 10 CMDs in $(B-V, M_V)$ and in $(g-r, M_g)$ using the transformation C08 for the same stars as in Fig. 6. The left panels show the Padua isochrones with $[\text{Fe}/\text{H}] = +0.13$ for the ZAMS and $[\text{Fe}/\text{H}] = -0.55$ at age 12 Gyr. The right panels show the Dartmouth isochrones with the same metallicities, respectively.

In the two-colour diagrams the picture is different. Here the new Padua ZAMS fit better than the old one, but the colour spread along the MS cannot be reproduced. For the Dartmouth isochrones there is a large offset at the young and metal rich end.

Finally we compare the ridge lines for the star clusters M71 and NGC 6791 of Clem et al. (2008) with isochrones. For M71 we use an age of 12 Gyr and $[\text{Fe}/\text{H}] = -0.55$. For the old metal rich cluster NGC 6791 we use an age of 8 Gyr and choose the closest available metallicity, which is $[\text{Fe}/\text{H}] = +0.2$ for Padua and $[\text{Fe}/\text{H}] = +0.44$ for Dartmouth. The results are shown in Figs. 13 and 14. Generally there is a better agreement of the Dartmouth isochrones with the ridge lines of the star clusters in $(g-r, M_g)$. The offsets of both sets of isochrones in $(r-i, M_r)$ are much larger with a similar systematics as for the local stellar sample. In the two-colour diagrams it becomes again obvious that the variation in colour due to metallicity spread is too small for F to K stars and too large in the M star regime.

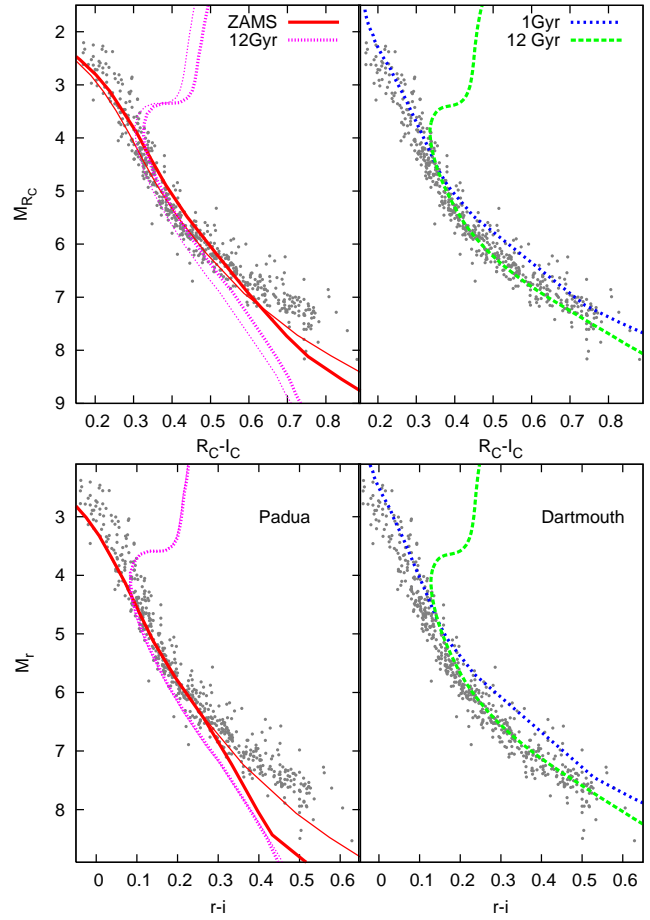


Fig. 11 CMDs in (R_C-I_C, M_{R_C}) and in $(r-i, M_r)$ with stars and isochrones as in Fig. 10.

7 Summary

We transformed the MS of F to K dwarfs in the solar neighbourhood from Johnson Cousins $B V R_C I_C$ to SDSS colours $g r i$ using the transformations of different authors. We used the complete sample of stars in a 25 pc sphere around the Sun from the Catalogue of Nearby Stars (CNS4) with Hipparcos distances to determine the mean MS properties in $(g-r, M_g)$ with the transformation C08 of Chonis & Gasca (2008). With the subsample, where all colours are available, we determined the mean MS in the CMDs in $(g-r, M_g)$ and $(r-i, M_r)$ and the two-colour diagram $(g-r, r-i)$. The systematic differences between the transformations of different authors in $M_g, M_r, g-r$ and $r-i$ are below 0.1 mag. In the cases, where $V-R_C$ is used in the transformations a considerable individual scatter up to 0.3 mag are introduced. This was not expected, when using more colour-terms in the transformations. The position of the mean MS in the CMDs is very sensitive to systematic deviations in the transformations. The differences in $M_g(g-r)$ are up to 0.5 mag and in $M_r(r-i)$ up to 0.3 mag, which is significant for photometric distance estimations. Also the 'bright' MS of Jurić et al. (2008) is consistent with the local stellar sample.

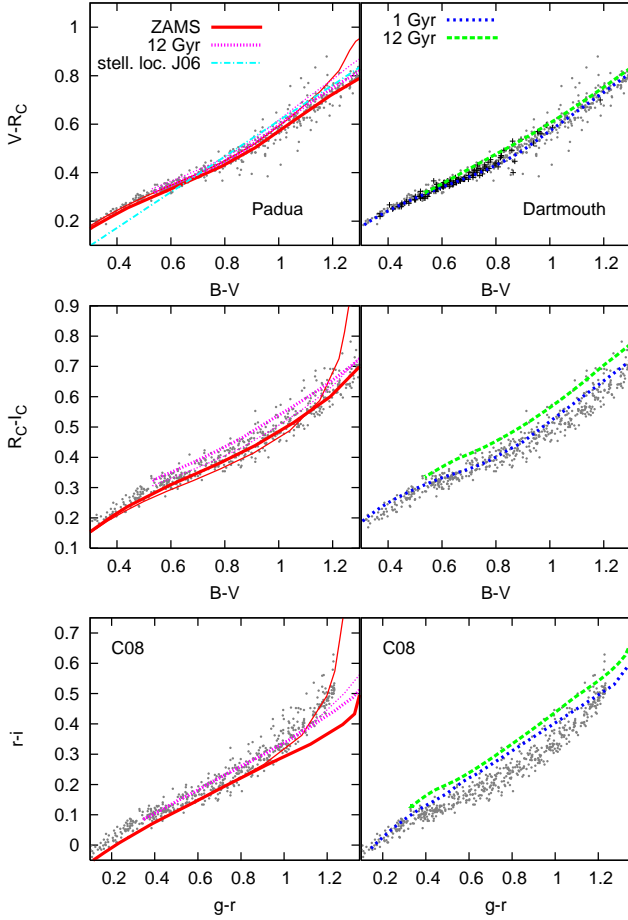


Fig. 12 2-colour diagrams of stars and isochrones as in Fig. 10. In the upper left panel the thin line shows the stellar locus, where the set of equations of J06 are consistent with each other. In the upper right panel the 119 stars with missing $R_C - I_C$ only are added (crosses).

The distribution of the solar neighbourhood stars in the CMDs and the two-colour diagram agree reasonably well with fiducial colour magnitude sequences of star clusters observed in $g' r' i'$. The best agreement occurs with the transformation C08 of Chonis & Gascall (2008).

The comparison with theoretical isochrones, especially in $(r - i, M_r)$ and $(g - r, r - i)$, is less satisfying. The systematic differences in shape and location require further calibration by observations in the SDSS filter system.

The solar neighbourhood provides a good testcase for the interpretation of mixed stellar populations. The results presented here can be used for detailed models of the Milky Way disc based on star counts, when extrapolated to the bright end in apparent magnitude. For this application we provide the local stellar number densities as function of colour $g - r$.

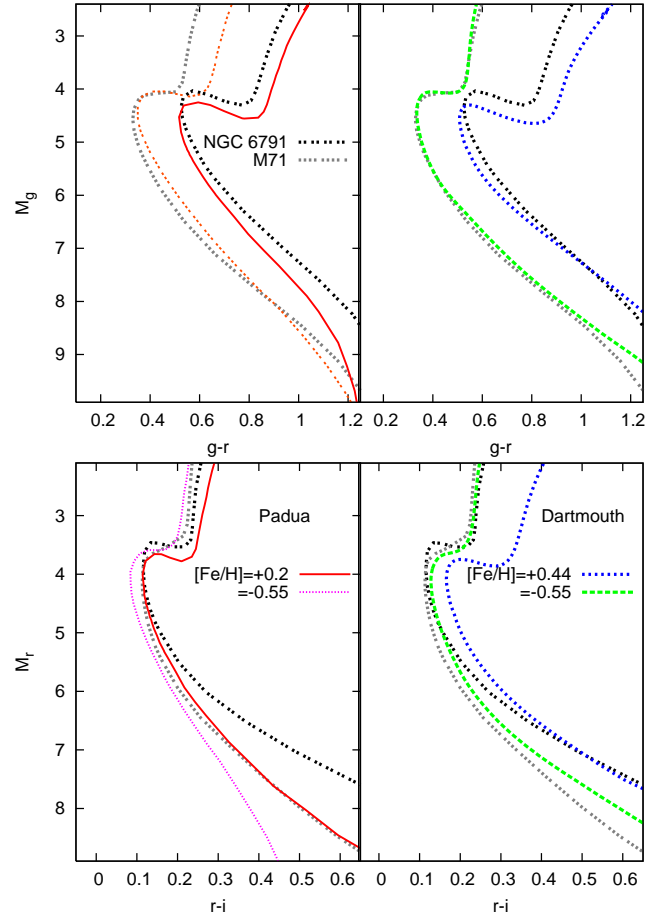


Fig. 13 Comparison of the fiducial star clusters NGC 6791 and M71 with the corresponding isochrones from Padua (left panels: 8 Gyr, $[\text{Fe}/\text{H}] = +0.2$ and 12 Gyr, $[\text{Fe}/\text{H}] = -0.55$) and Dartmouth (right panels: 8 Gyr, $[\text{Fe}/\text{H}] = +0.44$ and 12 Gyr, $[\text{Fe}/\text{H}] = -0.55$).

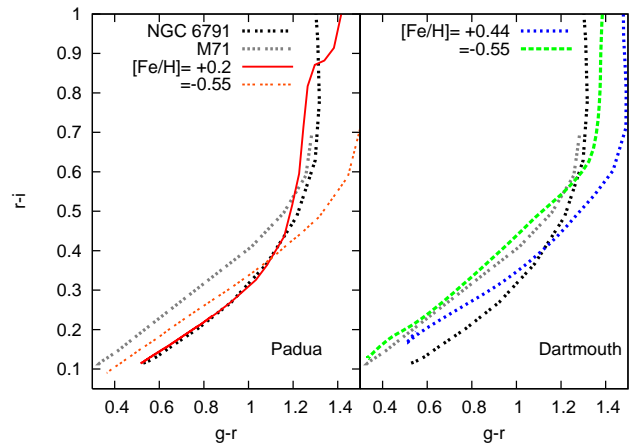


Fig. 14 Same cluster ridge lines and isochrones as in Fig. 13 in the 2-colour diagrams.

References

- Abazajian, K., Adelman-McCarthy, J. K., Agüeros, M.A. et al.: 2003, *AJ* 126, 2081
- Adelman-McCarthy, J. K., Agüeros, M.A., Allam, S.S. et al.: 2008, *ApJS* 175, 297
- Bilir, S., Karaali, S., Tunçel, S.: 2005, *AN* 326, 321
- Bilir, S., Ak, S., Karaali, S., Cabrera-Lavers, A., Chonis, T. S., Gaskell, C. M.: 2008, *MNRAS* 384, 1178
- Carraro, G., Villanova, S., Demarque, P., McSwain, M. V., Piotto, G., Bedin, L. R.: 2006, *ApJ* 643, 1151
- Chonis, T. S., Gaskell, C. M.: 2008, *AJ* 135, 264
- Cleveland, W., S., 1981:, *The American Statistician*, 35:54
- Clem, J. L., VandenBerg, D. A., & Stetson, P. B.: 2007, *AJ* 134, 1890
- Clem, J. L., VandenBerg, D. A., & Stetson, P. B.: 2008, *AJ* 135, 682
- Dotter, A., Chaboyer, B., Jevremović, D., Baron, E., Ferguson, J. W., Sarajedini, A., Anderson, J.: 2007, *AJ* 134, 376
- Dotter, A., Chaboyer, B., Jevremovic, D., Kostov, V., Baron, E., Ferguson, J. W.: 2008, *ApJS* accepted, astro-ph 0804.4473
- Fukugita, M., Ichikawa, T., Gunn, J. E., Doi, M., Shimasaku, K., Schneider, D. P.: 1996, *AJ* 111, 1748
- Girardi, L., Bertelli, G., Bressan, A., Chiosi, S., Groenewegen, M.A.T., Marigo, P., Salasnich, B., Weiss, A.: 2002, *A&A* 391, 195
- Girardi, L., Grebel, E. K., Odenkirchen, M., Chiosi, C.: 2004, *A&A*, 422, 205
- Ivezić, Ž., Smith, J.A., Miknaitis, G., et al.: 2007, *ASP Conf.* 464, 165
- Jahreiß H., Wielen R. 1997: In B. Battrock, M.A.C. Perryman, eds., *Proc. ESA SP-402 (Nordwijk, ESA)* 675
- Jordi, K., Grebel, E. K., Ammon, K.: 2006, *A&A* 460, 339
- Jurić, M., Ivezić, Ž., Brooks, A., et al.: 2008, *AJ* 673, 864
- Kyeong, J.-M., Byun, Y.-I., Chun, M.-S.: 1997, *JASS* 14, 194
- Landolt, A.U.: 1992, *AJ*, 104, 340
- Marigo, P., Girardi, L., Bressan, A., Groenewegen, M.A.T., Silva, L., Granato, G.L.: 2008, *A&A* 482, 883
- Padmanabhan, N., Schlegel, D.J., Finkbeiner, D.P. et al.: 2008, *ApJ* 674, 1217
- Rodgers, C. T., Canterna, R., Smith, J. A., Pierce, M. J., Tucker, D. L.: 2006, *AJ* 132, 989
- Schlegel, D. J., Finkbeiner, D. P., Davis, M.: 1998, *ApJ* 500, 525
- Smith, J. A., Tucker, D.L., Kent, S. et al.: 2002, *AJ* 123, 2121
- Stetson, P. B.: 2000, *PASP* 112, 925
- Tucker, D. L., Kent, S., Richmond, M.W. et al.: 2006, *AN* 327, 821
- VandenBerg, D. A., Clem, J. L.: 2003, *AJ* 126, 778